MNRAS **000**, 1–7 (2022) Preprint 9 November 2022 Compiled using MNRAS LATEX style file v3.0

Analytic Modelling of Binary-Single Encounters: Non-Thermal Eccentricity Distribution and Gravitational-Wave Source Formation

Yonadav Barry Ginat,[1]⋆ and Hagai B. Perets[1]
[1]*Faculty of Physics, Technion – Israel Institute of Technology, Haifa, 3200003, Israel*

arXiv:2205.15957v2 [astro-ph.HE] 8 Nov 2022

Accepted XXX. Received YYY; in original form ZZZ

ABSTRACT
Chaotic three-body interactions may lead to the formation of gravitational-wave sources. Here, by modelling the encounter as a series of close, non-hierarchical, triple approaches, interspersed with hierarchical phases, in which the system consists of an inner binary and a star that orbits it, we compute the pericentre probability distribution, and thereby the in-spiral probability in any given binary-single encounter. We then consider the indirect influence of binary-single encounters on the population of gravitational-wave sources, by changing the eccentricity distribution of hard binaries in clusters; we calculate this distribution analytically, by requiring that it be invariant under interactions with single stars.

Key words: galaxies: clusters: general – chaos – gravitational waves – (stars:) binaries (including multiple): close

1 INTRODUCTION

Chaotic three-body interactions are a dynamical pathway of gravitational-wave source production, especially in dense areas such as clusters (Hills 1975; Sigurdsson & Hernquist 1993; Quinlan 1996; Portegies Zwart & McMillan 2000; Rodriguez et al. 2015; Kocsis 2020; Safarzadeh 2020; Tagawa et al. 2020; Mandel & Broekgaarden 2022; Toonen et al. 2022). The rate of such phenomena is primarily determined by the probability that two of the three bodies approach each other sufficiently closely to coalesce within a dynamical time. Previous progress on the probabilistic understanding of the three-body problem is reviewed by(Valtonen & Karttunen 2006, and references therein); recently significant progress has been made (Stone & Leigh 2019; Kol 2021; Ginat & Perets 2021), particularly advancing the understanding of the role played by the total angular momentum, which opened the door to analytical modelling of the probability of such interactions leading to gravitational-wave in-spirals.

In this paper, we are concerned only with encounters of single stars with hard binaries, which lead to so-called resonant interactions, in which there is a time when all three bodies are in an approximate energy equipartition. As such an encounter proceeds as a series of hierarchical and non-hierarchical phases (Hut & Bahcall 1983; Anosova 1986; Anosova & Orlov 1986; Samsing et al. 2014), the probability of merging is determined by the probability distribution of the periapsis of the inner binary during a hierarchical phase, as well as the probability of close double approaches' occurring during a chaotic phase. As the initial binary is hard (i.e. its binding energy is much larger than the typical kinetic energy of a star in the cluster), it is necessarily the case that the interaction terminates when one of the three bodies is ejected to infinity (Arnold et al. 2006), or by a merger or a collision.

Besides dynamically forming gravitational-wave sources, which are discussed in §3, binary-single encounters also change the distribution of eccentricities in clusters: a binary's eccentricity typically changes considerably after each interaction with a single star; for an entire cluster, this process leads to a universal eccentricity distribution of hard binaries, which we endeavour to compute by studying the statistical solution of the non-hierarchical three-body problem in §4. We begin, however, by discussing the pericentre distribution in §2, which we then use in §3 to derive the in-spiral probability.

2 THE PERIAPSIS PROBABILITY DISTRIBUTION

The distribution of the orbital parameters of the remnant binary is (Ginat & Perets 2021)

$$f_b(E_b,\mathbf{S}|E,\mathbf{J})\ \mathrm{d}^2\mathbf{S}\mathrm{d}E_b \propto \frac{m_b\theta_{\max}(E_b,R,|\mathbf{J}-\mathbf{S}|)\ \mathrm{d}^2\mathbf{S}\mathrm{d}E_b}{|\mathbf{J}-\mathbf{S}|\,|E-E_b|^{3/2}\,|E_b|^{3/2}}.$$

⋆ E-mail: ginat@campus.technion.ac.il

© 2022 The Authors

(1)

Here, the binary energy is E_b, its angular momentum is $\mathbf{S}$, and its mass is m_b. The total, three-body energy is E and the angular momentum is $\mathbf{J}$. We approximate $\theta_{\max}$ by $\theta_{ap}\sqrt{1-b^2}(1+2b^2)$, with b defined in equation (A7) of Ginat & Perets (2021). Quantities with a subscript b refer to the remnant binary, and likewise a subscript s refers to the orbit of the ejected star about this binary. Below we denote the total three-body mass by M. R is the minimum distance the third body might have relative to the leftover binary's centre of mass, and still be in a hierarchical orbit; it is defined in equation (10) of Ginat & Perets (2021).

Below we will mostly be concerned with the marginal distribution of E_b, and the binary's periapsis, r_p, chiefly at small values of r_p. This means that we should integrate f_b, multiplied by the Dirac delta function $\delta\left(r_p-a_b(1-e_b)\right)$, over $\mathbf{S}$; but first, let us derive the joint eccentricity and semi-major axis distribution. This is done by integrating over the direction of $\mathbf{S}$, i.e. over the inclination. Let us define the auxiliary function

$$\psi(x)=\frac{1}{4}\left(x\sqrt{1-x^2}\left(1+2x^2\right)+3\arcsin x\right); \tag{2}$$

integration over the direction of $\mathbf{S}$ yields,

$$f_b(E_b,S|E,\mathbf{J})\,\mathrm{d}S\mathrm{d}E_b\propto\frac{m_b\theta_{ap}(E_b,R)\,\mathrm{d}S\mathrm{d}E_b}{|E-E_b|^{3/2}\,|E_b|^{3/2}}\times\frac{A_p}{J}\Delta\psi, \tag{3}$$

where $A_p=\mu_s\sqrt{GMR}\sqrt{2\pm\frac{R}{a_s}}$ (the negative sign for ejection on a bound orbit, and *vice versa*), and

$$\Delta\psi\equiv\psi\left(\min\left\{\frac{J+S}{A_p},1\right\}\right)-\psi\left(\min\left\{\frac{|J-S|}{A_p},1\right\}\right), \tag{4}$$

provided that $J_m\le J\le J_M$, with $J_m\equiv A_pj_m\equiv\max\{0,S-\alpha\}$ and $J_M\equiv A_pj_M\equiv\min\{J_{\max},\alpha+S\}$, where

$$\alpha\equiv\begin{cases}A_p, & \text{unbound}\\ \min\left\{A_p,\mu_s\sqrt{GMR\eta\left(2-\eta\frac{R}{a_s}\right)}\right\}, & \text{bound.}\end{cases} \tag{5}$$

At small $S\ll J,A_p$,

$$\Delta\psi\approx 2S\sqrt{1-\frac{J^2}{A_p^2}}\left(1+2\frac{J^2}{A_p^2}\right). \tag{6}$$

On the other hand, for small S,J, with $S>J$, one has $\Delta\psi\approx 2J/A_p$.

There are two possibilities: if J is itself small, one expects a super-thermal eccentricity distribution (Stone & Leigh 2019), while for other values of J, it should become approximately thermal. At any rate, the pericentre distribution is given by

$$\begin{aligned}f_b(r_p|E,\mathbf{J})&=\iint f_b(E_b,S|E,\mathbf{J})\delta\left(r_p-a_b(1-e_b)\right)\,\mathrm{d}S\mathrm{d}E_b\\&\equiv\int f_b(r_p,E_b|E,\mathbf{J})\,\mathrm{d}S.\end{aligned} \tag{7}$$

Let us approximate $f_b(r_p,E_b|E,\mathbf{J})$ for small values of r_p (corresponding to high eccentricities, or small S), in the two afore-mentioned possibilities. First, if J is not small relative to A_p, we find

$$\begin{aligned}f_{b,1}(r_p,E_b|E,\mathbf{J})\propto&\frac{e_b}{\mu_b}\frac{\theta_{ap}J_c^2\Theta(a_b-r_p)}{J\sqrt{|E_b|}\,|E-E_b|^{3/2}}\\&\times\sqrt{1-\frac{J^2}{A_p^2}}\left(1+2\frac{J^2}{A_p^2}\right),\end{aligned} \tag{8}$$

while for $J\ll A_p$, $S>J$,

$$f_{b,2}(r_p,E_b|E,\mathbf{J})\propto\frac{e_b}{\mu_b}\frac{\theta_{ap}J_c\Theta(a_b-r_p)}{\sqrt{|E_b|}\,|E-E_b|^{3/2}}\frac{2}{\sqrt{1-e_b^2}}, \tag{9}$$

where $e_b=1-r_p/a_b$.

3 THE IN-SPIRAL PROBABILITY

The time to coalescence of a binary, due to gravitational-wave emission, is (e.g. Maggiore 2008, and references therein)

$$\tau(a_b,e_b)=\tau_0(a_b)(1-e_b)^{7/2}g(e_b), \tag{10}$$

where

$$\tau_0(a_b)=\frac{5}{256}\frac{c^5a_b^4}{G^3m_b^2\mu_b} \tag{11}$$

is the time to coalescence of a circular binary with initial semi-major axis a_b, and $g(e_b)$ is a slowly-varying function of e_b, that starts at 1 at $e_b=0$, and reaches $\frac{768}{425}$ at $e_b=1$. Henceforth, we approximate $g(e_b)\approx 1$.

There are two possibilities for a gravitational-wave merger to be caused by a binary-single encounter:

(i) During a chaotic phase, one of the stars passes so close to another that some energy is radiated in gravitational waves, leaving the two as a soon-to-merge binary, while the third object is in a hierarchical orbit about it. The probability for this is (Hut & Inagaki 1985; Ginat & Perets 2021) $p_{\mathrm{gw,3b}}=\frac{12a_0r_0}{R^2}$, where r_0 is the maximum possible distance of closest approach between the two stars that would merge, for the merging to occur in a dynamical time, and a_0 is the original semi-major axis.

(ii) One of the stars is ejected from the triple at the end of a chaotic phase, and the orbital parameters of the remnant binary yield a τ which is smaller than the orbital period of the outer binary (i.e. the inner binary merges before the third body returns).

We therefore need to solve $\tau_{\mathrm{dyn}}\ge\tau(a_b,e_b)$, with

$$\tau_{\mathrm{dyn}}\equiv 2\pi\frac{a_s^{3/2}}{\sqrt{GM}}. \tag{12}$$

One can rearrange this inequality to the form $r_p\le r_0(a_b)$, where

$$r_0\equiv a_b\min\left\{1,\left|1-\sqrt{1-\left(\frac{256G^3m_b^2\mu_b\tau_{\mathrm{dyn}}}{5c^5a_b^4}\right)^{2/7}}\right|\right\}. \tag{13}$$

Let $\mathcal{M}$ be the region in (E_b,r_p)-space where $\tau_{\mathrm{dyn}}\ge\tau$; because gravitational-wave emission is weak, $\mathcal{M}$ has a small probability. Furthermore, let us define $p_{\mathrm{gw,bd}}\equiv P(\mathcal{M}|\mathrm{bound})$, i.e. the probability of having an inner binary whose orbital parameters satisfy $\tau_{\mathrm{dyn}}\ge\tau(a_b,e_b)$, given that

the third body is ejected on a bound orbit. If we further neglect any losses of total energy and angular momentum (save for those occurring during a merger), then the random-walk model of Ginat & Perets (2021) predicts that the probability for a gravitational-wave merger to occur is

$$P_{\rm gw} = 1 - \left[\sum_{n=1}^{\infty} p_{\rm ubd} p_{\rm bd}^{n-1}(1-p_{\rm gw,3b,ubd}) \times (1-p_{\rm gw,3b,bd})^{n-1}(1-p_{\rm gw,bd})^{n-1}\right] = 1 - \frac{p_{\rm ubd}(1-p_{\rm gw,3b,ubd})}{1-p_{\rm bd}(1-p_{\rm gw,bd})(1-p_{\rm gw,3b,bd})}. \quad (14)$$

Here, $p_{\rm ubd} = 1 - p_{\rm bd}$ is the probability of ejecting the third body to infinity, $p_{\rm gw,3b,ubd}$ is the afore-mentioned probability of having a gravitational-wave merger during the chaotic phase, leading to an unbound un-merged body (and similarly for $p_{\rm gw,3b,bd}$). We don't have a $p_{\rm gw,ubd}$, as once the encounter concludes with an ejection, we strictly do not consider any subsequent gravitational-wave merger of the remnant binary as one dynamically caused by a triple encounter.

If all the merging probabilities are very small, and if, barring gravitational-wave emission, there are $\langle N\rangle = \frac{1}{p_{\rm ubd}}$ chaotic phases until an ejection, the cross-section for a gravitational-wave merger in one of the two channels is

$$\sigma_{\rm gw} \approx \langle N\rangle \left[12 a_0 \mathbb{E}\left(\frac{r_0(a_b)}{R^2}\right) + p_{\rm gw,bd}\right]\sigma_{\rm tot}, \quad (15)$$

$P_{\rm gw}$ is plotted in figure 1, and compared with the simulations of Samsing et al. (2014). One can see that these results are in broad agreement with those of Ginat & Perets (2021), who found $\beta \approx 1.3$, $\eta \approx 5$ to agree with the numerical data. The mild discrepancy between 1.3 and 1.5 is probably mostly due to the somewhat simplistic nature of the effective tidal model for energy losses adopted by that work, relative to the one incorporated in the numerical simulations, as well as the linear approximation (in the probability of significant tidal interactions, $12 a_0 r_0/R^2$) used there, which induces an error in β of the order of $12 r_0/(\beta a_0) \approx 0.25$. We use $\beta = 1.5$ and $\eta = 5$ in this paper, unless stated otherwise. We also plot, in figure 2, the gravitational-wave in-spiral probability for various mass configurations.

To conclude this section, we present a plot of $\langle N\rangle$ as a function of the initial conditions, for equal masses in figure 3. Being dimension-less, it can only depend on the total energy and angular momentum in the combination $EJ^2/(\mu_s^3 G^2 M^2)$ (and on mass-ratios), but it is extremely sensitive to the total angular momentum. Indeed, when the total angular momentum is too large, it is impossible for the system to be in the strong-interaction region of phase-space, and $f_b = 0$ (Stone & Leigh 2019; Ginat & Perets 2021). This is manifested by the probability for ejecting the third body to infinity on an unbound orbit occupying a smaller fraction of the probability mass, relative to the probability of ejecting it on a bound trajectory (which also decreases), as J increases, until, at some value J_*, both vanish; in figure 3 this occurs at $|E|\,J^2/(\mu_s^3 G^2 M^2) \approx 1.37$, but the validity of treating the encounter as a highly-chaotic one becomes moot already at $|E|\,J^2/(\mu_s^3 G^2 M^2) \gtrsim 1.2$. Indeed, a numerical study by Parischewsky et al. (2021) found that, for two-dimensional scattering processes, the system is most chaotic

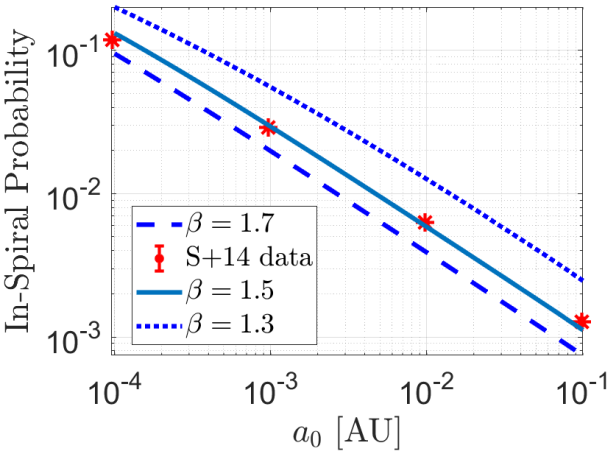


Figure 1. The gravitational-wave in-spiral/collision probability as a function of the initial semi-major axis. The particles are three 1 $M_\odot$ black holes, and the in-coming star's velocity is 10 km s^{-1}. The prediction of equation (14), for $\eta = 5$ and various values of β, is plotted in blue and compared with the numerical results of Samsing et al. (2014) in red.

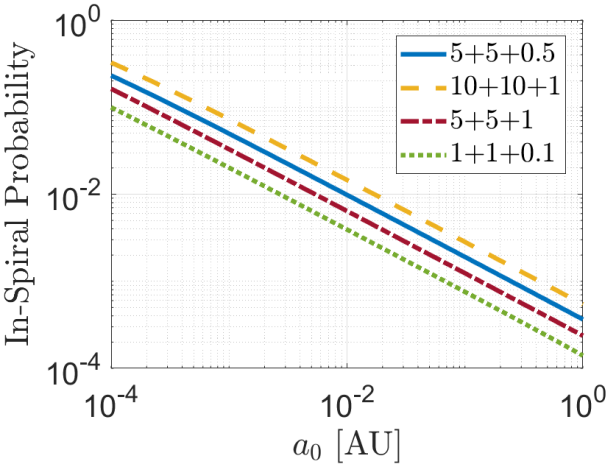


Figure 2. The same as figure 1, but with various masses.

when $J = 0$. In future work we will use this computation of $\langle N\rangle$ as a function of the angular momentum to derive the life-time distribution of a resonant encounter.

Having computed the probability for one binary's interaction with one single star to produce a gravitational-wave in-spiral, we now turn to another possibility – that interactions with many single stars will shape the eccentricity distribution of the entire cluster, in a way that may be favourable to the emergence of gravitational-wave sources.

4 MULTIPLE ENCOUNTERS IN CLUSTERS

After many encounters with single stars, one would expect the probability distribution of the eccentricities of binaries in a cluster to reach some steady-state distribution, which we

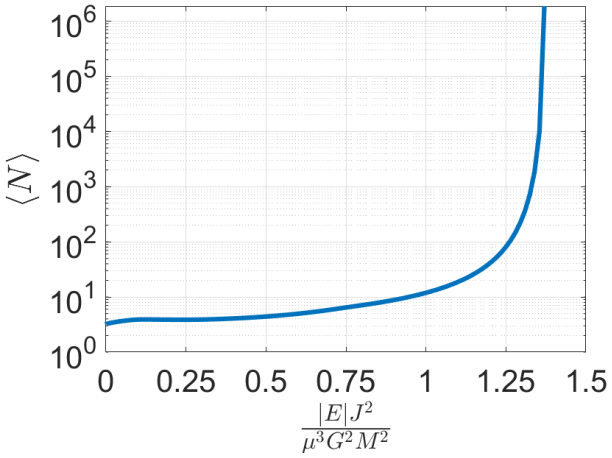


Figure 3. A plot of $\langle N \rangle$ as a function of the conserved quantities.

denote by $f(E_b, \mathbf{S})$. Of course, the energy distribution of binaries does not, in general, reach a steady-state distribution, by Heggie's law (Heggie 1975; Binney & Tremaine 2008), but the eccentricity distribution does: after every encounter, the eccentricity effectively randomises (Stone & Leigh 2019), according to some distribution set by the total energy and angular momentum. If the remnant binary turns out to have a very high eccentricity, then it is probable that the eccentricity will be lower after the next one. The converse is also true, and therefore one expects the eccentricity distribution of many binaries in a cluster to tend towards some steady state. As the eccentricity varies considerably from one encounter to the next, this approach is much faster than the gradual hardening process, so one may treat the latter as adiabatic. A different approach to describe the evolution of the distribution of orbital parameters of binaries in clusters is pursued by Leigh et al. (2022), with which the reader may compare our results.

The steady-state distribution must satisfy

$$f(E_b, \mathbf{S}) = \int \mathrm{d}E \mathrm{d}^2\mathbf{J} f_b(E_b, \mathbf{S}|E, \mathbf{J}) p(E, \mathbf{J}), \tag{16}$$

where $p(E, \mathbf{J})$ is the probability distribution of the total energy and angular momentum. For single stars that can come in from any direction, and at any impact parameter, the probability of finding $\mathbf{J}$ is approximately independent of the binary's previous angular momentum. Besides, as the binary is hard, E is approximately equal to the binary's initial energy. Then,

$$f(E_b, S) = \int \mathrm{d}E \iint_0^{J_{\max}(E)} \frac{J \mathrm{d}J \mathrm{d}\phi_J}{\pi J_{\max}^2(E)} f_b(E_b, S|E, \mathbf{J}) f(E), \tag{17}$$

where (J, ϕ_J) are the polar co-ordinates of $\mathbf{J}$, and

$$f(E) = \int \mathrm{d}S f(E, S). \tag{18}$$

Assuming that $J_{\max}(E) + S \leq A_p$, we find that

$$\iint_0^{J_{\max}(E)} \frac{J \mathrm{d}J \mathrm{d}\phi_J}{\pi J_{\max}^2(E)} f_b(E_b, S|E, \mathbf{J}) \tag{19}$$

$$\propto \frac{2A_p^2}{J_{\max}^2(E)} \frac{m_b \theta_{ap}(E, E_b, R) \Delta\phi}{|E - E_b|^{3/2} |E_b|^{3/2}}, \tag{20}$$

where

$$\begin{aligned}
\Delta\phi(E, S) \equiv{}& \Theta\left(1 - S - \frac{J_{\max}}{A_p}\right) \Big[\phi(j_M + s) - \phi(s) + \phi(0) \\
&+ \phi(\max\{s - j_M, 0\}) - \phi(\max\{j_M - s, 0\}) - \phi(s - j_m)\Big] \\
&+ \Theta(s - 1) \Big[\psi(1)(j_M - j_m) + \phi(0) + \phi(\max\{s - j_M, 0\}) \\
&- \phi(\max\{j_M - s, 0\}) - \phi(s - j_m)\Big] \\
&+ \Theta(1 - s)\Theta\left(s + \frac{J_{\max}}{A_p} - 1\right) \Big[\phi(1) - \phi(s) \\
&+ \psi(1)(j_M - j_c) + \phi(0) + \phi(\max\{s - j_M, 0\}) \\
&- \phi(\max\{j_M - s, 0\}) - \phi(s - j_m)\Big].
\end{aligned} \tag{21}$$

with $\phi(u)$ defined in equation (A12) of Ginat & Perets (2021), $s \equiv S/A_p$, $j_M \equiv \min\{J_{\max}/A_p, \alpha/A_p + s\}$, $j_m \equiv \max\{0, s - \alpha/A_p\}$, and Θ denoting the Heaviside theta function. Equation (21) is derived in appendix A. The maximum angular momentum is set by the requirement, that when the initial angular momenta of the in-coming star and the binary are aligned, the farthest distance of closest approach of the star and the centre-of-mass of the binary be equal to the latter's semi-major axis. This yields

$$J_{\max} = \sqrt{2GM} \max\left\{\mu_n \sqrt{R_n}\right\}_{n=1}^{3}, \tag{22}$$

where n refers to the identity of the ejected particle, and R_n is defined by equation (10) of Ginat & Perets (2021), evaluated for the case where star n is ejected, at a_b which gives E_b equal to the total three-body energy.

To find an analytical approximation of $f(E_b, S)$, we lastly assume that $f(E)$ is sharply peaked about some value E_*, so that eventually

$$f(E_b, S) \propto \frac{2m_b A_p^2}{J_{\max}^2(E_*)} \frac{\theta_{ap}(E_*, E_b, R) \Delta\phi(E_*, S)}{|E_* - E_b|^{3/2} |E_b|^{3/2}}. \tag{23}$$

One requires additional information to determine E_*, *viz.* the current mean binding energy of binaries in the cluster.

The difference between f and f_b arises chiefly because while the latter is constrained by the total angular momentum, the former isn't, so its expression is actually simpler than that of f_b. The marginal probability distribution of f is not thermal (and likewise for f_b, as shown by Stone & Leigh 2019); it is somewhat super-thermal, as can be seen from figure 4. The reason that this distribution is super-thermal is that $\Delta\psi$ in equation (4) can yield either a thermal distribution (for large J, equation 6) or a super-thermal one (for small J). So, when integrating over all allowed values of J, one has a convex combination of (close to) thermal distributions and super-thermal ones, to various degrees, which results in (23).

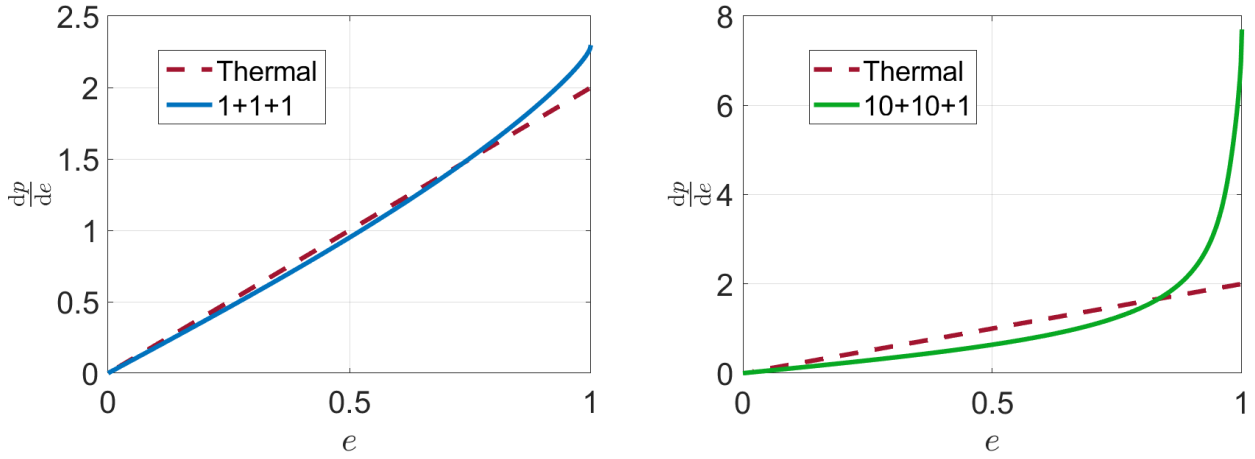


Figure 4. The marginal eccentricity distribution (normalised) arising from integrating equation (23) over energies numerically, and changing from S to e_b, compared with a thermal distribution (dashed line). The three bodies' masses are equal on the left panel, while they are 10 $M_\odot$ in the binary, with a single perturber of 1 $M_\odot$, on the right panel.

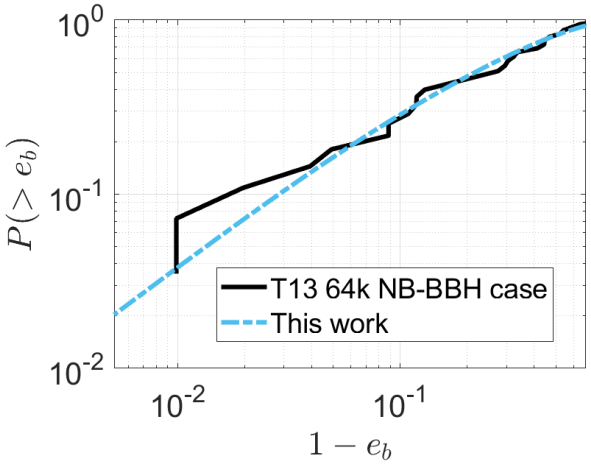


Figure 5. The marginal eccentricity distribution arising from integrating equation (23) over energies numerically, and changing from S to e_b, compared with numerical data from the 64k case (largest number of particles) of figure 8 of Tanikawa (2013).

Perhaps one might have expected f to be a thermal distribution, based on the following (erroneous) reasoning: for a binary in thermal equilibrium, we know that the distribution of eccentricities is thermal. 'Collisions' with single stars should allow for efficient energy and angular-momentum mixing, and therefore is expected to drive the distribution towards a thermal one. However, as we've shown here, these very encounters drive f towards a distribution which is non-thermal; the reason is, of course, that (hard) binaries can never be in thermal equilibrium in a cluster that contains single stars, as already attested to by Heggie's law.

The results in this section, pertain to the single-mass case, where all stars in a cluster are of the same mass; of course, multi-mass multiple encounters are also possible in realistic clusters. Suppose, for example, that there are two types of astral objects in a cluster: a massive compact object, and a lighter star. Then, as time goes by, an ever increasing fraction of the binary population will be composed of two compact objects (as there is always an overwhelming probability to eject the lighter particle of the three; e.g. Saslaw et al. 1974; Hills 1992; Heggie et al. 1996; Ginat & Perets 2021; Manwadkar et al. 2020; Kol 2021; Manwadkar et al. 2021), while the singles may contain both. If one assumes that this is the case, then one may use the formulæ of §4 straightforwardly. We show an example of this in figure 4, which is different from the equal-mass case. In figure 5 we compare these predictions to the numerical result of Tanikawa (2013), which considered the eccentricity distribution of tight black hole binaries that were dynamically ejected from a globular cluster, simulated by an N-body code. Our prediction that is plotted there is for $m_1 = m_2 = 10\ M_\odot$ (close to the most likely binary component masses found there), with a perturber with mass $m \geq 1\ M_\odot$ distributed according to the mass function of Tanikawa (2013).[1] We expect the hard binaries that remain in the cluster to have a similar distribution after a sufficiently long time, and likewise for gravitational-wave source candidates. However, as shown by Geller et al. (2019), most binaries in clusters have not yet reached this stage, and their distribution is closer to the sub-thermal initial condition (see Duchêne & Kraus 2013; Moe & Stefano 2017 for observational evidence); besides, collisions, coupled to diffusion by weak encounters, can also act to deplete the high-eccentricity tail of the distribution (e.g. Leigh et al. 2022).

5 CONCLUSIONS

The purpose of this paper is to provide an analytical formula for the probability distribution of the pericentre of a binary created by a close triple interaction, and to use it to compute the probability for a dynamically-generated

[1] Perturbers with mass $m \lesssim 1\ M_\odot$ were not included, since it is extremely unlikely that an interaction with a lighter star will eject the binary.

gravitational-wave in-spiral, engendered in this way. The result is given by equation (14). Here, we have been treating the three objects as point particles, but this is of course only true approximately. Indeed, at least when one of the particles is a star (i.e. not a compact object), collisions might be important (e.g. Hut & Inagaki 1985; Davies et al. 1993; Leigh et al. 2017); besides, here we considered only mergers, that occur during the three-body evolution, as dynamically-generated ones, but of course the final periapsis may be sufficiently small, that the remnant binary may merge before the next encounter (Samsing et al. 2022).

We have also shown how to compute the probability distribution of finding a hard binary with a given eccentricity, chosen at random from a cluster, when one takes into account multiple encounters with single stars. This distribution, equation (23) was found to be somewhat super-thermal, which is important for estimating the over-all rates of gravitational-wave in-spirals (Kocsis 2020; Mandel & Broekgaarden 2022), especially in gas-assisted mergers (Rozner & Perets 2022).

Observational evidence seems to suggests an eccentricity distribution of binaries which is shallower than the thermal one Duchêne & Kraus (2013); Moe & Stefano (2017); an intriguing possibility is that it is this discrepancy originates from a mass-and-number-weighted superposition of the distributions shown in figure 4 and described in §4.

ACKNOWLEDGEMENTS

We wish to thank Nathan Leigh for helpful comments. Y.B.G. is grateful for the support of the Adams Fellowship Programme of the Israeli Academy of Sciences and Humanities.

DATA AVAILABILITY

The data underlying this article will be shared on reasonable request to the corresponding author.

REFERENCES

Anosova J. P., 1986, Ap&SS, 124, 217
Anosova Z. P., Orlov V. V., 1986, Soviet Ast., 30, 380
Arnold V. I., Kozlov V. V., Neishtadt A. I., 2006, Mathematical aspects of classical and celestial mechanics, third edn. Encyclopaedia of Mathematical Sciences Vol. 3, Springer-Verlag, Berlin
Binney J., Tremaine S., 2008, Galactic Dynamics: Second Edition. Princeton University Press
Davies M. B., Benz W., Hills J. G., 1993, ApJ, 411, 285
Duchêne G., Kraus A., 2013, Annual Review of Astronomy and Astrophysics, 51, 269
Geller A. M., Leigh N. W. C., Giersz M., Kremer K., Rasio F. A., 2019, ApJ, 872, 165
Ginat Y. B., Perets H. B., 2021, Physical Review X, 11, 031020
Heggie D. C., 1975, MNRAS, 173, 729
Heggie D. C., Hut P., McMillan S. L. W., 1996, ApJ, 467, 359
Hills J. G., 1975, AJ, 80, 809
Hills J. G., 1992, AJ, 103, 1955
Hut P., Bahcall J. N., 1983, ApJ, 268, 319
Hut P., Inagaki S., 1985, ApJ, 298, 502
Kocsis B., 2020, Dynamical Formation of Merging Stellar-Mass Binary Black Holes. Springer Singapore, Singapore, pp 1–44, doi:10.1007/978-981-15-4702-7˙15-1, https://doi.org/10.1007/978-981-15-4702-7_15-1
Kol B., 2021, Celestial Mechanics and Dynamical Astronomy, 133, 17
Leigh N. W. C., Geller A. M., Shara M. M., Garland J., Clees-Baron H., Ahmed A., 2017, MNRAS, 471, 1830
Leigh N. W. C., Stone N. C., Webb J. J., Lyra W., 2022, MNRAS,
Maggiore M., 2008, Gravitational Waves. Vol. 1: Theory and Experiments. Oxford Master Series in Physics, Oxford University Press
Mandel I., Broekgaarden F. S., 2022, Living Reviews in Relativity, 25, 1
Manwadkar V., Trani A. A., Leigh N. W. C., 2020, MNRAS, 497, 3694
Manwadkar V., Kol B., Trani A. A., Leigh N. W. C., 2021, MNRAS, 506, 692
Moe M., Stefano R. D., 2017, The Astrophysical Journal Supplement Series, 230, 15
Parischewsky H. D., Ceballos G., Trani A. A., Leigh N. W. C., 2021, arXiv e-prints, p. arXiv:2108.06335
Portegies Zwart S. F., McMillan S. L. W., 2000, ApJ, 528, L17
Quinlan G. D., 1996, New Astronomy, 1, 35
Rodriguez C. L., Morscher M., Pattabiraman B., Chatterjee S., Haster C.-J., Rasio F. A., 2015, Phys. Rev. Lett., 115, 051101
Rozner M., Perets H. B., 2022, arXiv e-prints, p. arXiv:2203.01330
Safarzadeh M., 2020, The Astrophysical Journal, 892, L8
Samsing J., MacLeod M., Ramirez-Ruiz E., 2014, ApJ, 784, 71
Samsing J., et al., 2022, Nature, 603, 237
Saslaw W. C., Valtonen M. J., Aarseth S. J., 1974, ApJ, 190, 253
Sigurdsson S., Hernquist L., 1993, Nature, 364, 423
Stone N. C., Leigh N. W. C., 2019, Nature, 576, 406
Tagawa H., Haiman Z., Kocsis B., 2020, The Astrophysical Journal, 898, 25
Tanikawa A., 2013, MNRAS, 435, 1358
Toonen S., Boekholt T. C. N., Portegies Zwart S., 2022, A&A, 661, A61
Valtonen M., Karttunen H., 2006, The Three-Body Problem. Cambridge University Press, Cambridge

APPENDIX A: DERIVATION OF $\Delta\phi$

To integrate over the angular momentum, we need to integrate equation (4) over J, from $J_m \equiv A_p j_m = \max\{0, S-\alpha\}$ to $J_M \equiv A_p j_M \equiv \min\{J_{\max}, \alpha+S\}$. Note, that $S - J_m \leq A_p$, and since $J_m \leq S$, $|S-J_m| \leq A_p$. In §4 we only need the unbound case. As J increases from J_m to S, this absolute value decreases to 0. Then, from $J=S$ to J_M, $|J-S|$ increases from 0 to $J_M - S \leq A_p$. Consequently,

$$\min\left\{\frac{|J-S|}{A_p}, 1\right\} = \frac{|J-S|}{A_p} \tag{A1}$$

over the entire allowed range of J. There are now three cases: $S > A_p$, $S \leq A_p$ but $S + J_{\max} > A_p$, and $S + J_{\max} \leq A_p$.

A1 Case $S > A_p$

Equation (4) reduces to

$$\psi(1) - \psi(|j-s|), \tag{A2}$$

where $j \equiv J/A_p$. We need to integrate

$$\Delta\phi = \int_{j_m}^{j_M} [\psi(1) - \psi(|j-s|)]\,\mathrm{d}j \tag{A3}$$

$$= \psi(1)(j_M - j_m) - \int_{j_m}^{\min\{s,j_M\}} \psi(s-j)\mathrm{d}j \tag{A4}$$

$$- \int_{s}^{\max\{j_M,s\}} \psi(j-s)\mathrm{d}j \tag{A5}$$

$$= \psi(1)(j_M - j_m) + \phi(0) - \phi(s-j_m) \tag{A6}$$

$$- \phi(\max\{j_M - s, 0\}) + \phi(\max\{0, s - j_M\}). \tag{A7}$$

A2 Case $S \leq A_p$ But $S + J_{\max} > A_p$

Now equation (4) yields

$$\psi(\min\{s+j, 1\}) - \psi(|s-j|). \tag{A8}$$

Observe that if $S \leq A_p$, $J_m = 0$; on the other hand, it is also true that if $J_m + S < A_p$, then $S \leq A_p$, so $J_m = 0$.

Let $j_c \equiv 1 - s$, whence by definition

$$0 = j_m \leq j_c \leq J_{\max}/A_p \leq j_M. \tag{A9}$$

The second integral, of $\psi(|s-j|)$, is the same as above. The first is

$$\int_{j_m}^{j_M} \psi(\min\{s+j,1\})\mathrm{d}j = \int_{0}^{j_M} \psi(\min\{s+j,1\})\mathrm{d}j \tag{A10}$$

$$= \int_{0}^{j_c} \psi(s+j)\mathrm{d}j + \psi(1)(j_M - j_c) \tag{A11}$$

$$= \phi(1) - \psi(s) + \psi(1)(j_M - j_c). \tag{A12}$$

Together with the second term, we find

$$\Delta\phi = \phi(1) - \psi(s) + \psi(1)(j_M - j_c) + \phi(0) - \phi(s - j_m) \tag{A13}$$

$$- \phi(\max\{j_M - s, 0\}) + \phi(\max\{0, s - j_M\}). \tag{A14}$$

A3 Case $S + J_{\max} \leq A_p$

In this case, since $J_{\max} \leq A_p - S \leq A_p + S$, the upper limit is $J_M = J_{\max}$. As before, $J_m = 0$. Then it is always the case that $s + j \leq 1$, so

$$\Delta\psi = \psi(s+j) - \psi(|s-j|). \tag{A15}$$

Performing the integrations yields

$$\Delta\phi = \phi(s + j_M) - \phi(s) + \psi(1)(j_M - j_c) + \phi(0) - \phi(s - j_m) \tag{A16}$$

$$- \phi(\max\{j_M - s, 0\}) + \phi(\max\{0, s - j_M\}). \tag{A17}$$

This paper has been typeset from a TEX/LATEX file prepared by the author.